

Novel platinum pyridinehydroxamic acid complexes: Synthesis, characterisation, X-ray crystallographic study and nitric oxide related properties

Darren Griffith^a, Alberta Bergamo^b, Sara Pin^b, Marta Vadori^c,
Helge Müller-Bunz^d, Gianni Sava^{b,c}, Celine J. Marmion^{a,*}

^a Centre for Synthesis and Chemical Biology, Department of Pharmaceutical and Medicinal Chemistry,
Royal College of Surgeons in Ireland (RCSI), 123 St. Stephen's Green, Dublin 2, Ireland

^b Fondazione Callerio, Via A. Fleming 22-31, I-34127 Trieste, Italy

^c Department of Biomedical Sciences, University of Trieste, Via L. Giorgieri 7-9, 34127 Trieste, Italy

^d School of Chemistry and Chemical Biology, University College Dublin, Belfield, Dublin 4, Ireland

Received 22 January 2007; accepted 7 March 2007

Available online 15 March 2007

Abstract

Herein, we describe the synthesis and characterisation of a novel class of Pt^{II} and Pt^{IV} pyridinehydroxamic acid (pyhaH) complexes of general formula *cis*-[Pt^{II}Cl₂(*x*-pyhaH)₂] and *cis*-[Pt^{IV}Cl₄(*x*-pyhaH)₂], respectively (where *x* = 3 or 4) in which the pyridinehydroxamic acid is coordinated to the platinum ion *via* the pyridine nitrogen only leaving the hydroxamic acid free to potentially release cytotoxic nitric oxide (NO). The crystal structure of the Pt^{IV} derivative, *cis*-[PtCl₄(4-pyhaH)₂] · 2CH₃OH is reported. To establish the biological effect of the uncoordinated hydroxamic acid moiety in the Pt^{II} compounds synthesised, the corresponding pyridinecarboxylic acid (pycaH) complexes of general formula *cis*-[Pt^{II}Cl₂(*x*-pycaH)₂] (where *x* = 3 or 4) and the Pt^{II} pyridine (py) complex, *cis*-[Pt^{II}Cl₂(py)₂] were synthesised and served as reference standards. The NO-releasing properties of each of the Pt^{II} compounds, the pyhaH and the pycaH ligands were studied. The Pt^{II} pyridinehydroxamic acid derivatives were found to induce potent *in vitro* effects attributable to either NO-release from the hydroxamic acid moiety and/or stimulation of inducible nitric oxide synthase of endothelial cells.

© 2007 Elsevier Ltd. All rights reserved.

Keywords: Platinum; Hydroxamic acids; Nitric oxide; Nitric oxide synthase; Guanylate cyclase; Vascular relaxation

1. Introduction

Cancer is one of the most complex and deadly diseases known to man. Although today nearly 50% of all anti-cancer therapies are platinum (Pt)-based [1], surprisingly to date only three Pt drugs have been approved for worldwide clinical use, namely cisplatin, carboplatin and oxaliplatin, Fig. 1 while three others, nedaplatin, heptaplatin and lobaplatin, Fig. 1, have been approved only in Japan, South Korea and China, respectively [1,2]. The cytotoxicity

of Pt drugs is attributed to their ability to bind DNA and induce apoptosis [1,2]. There are drawbacks however associated with their use (such as their limited activity against many common human cancers, their susceptibility to acquired drug resistance and their toxicity) which limits their widespread application and efficacy. The search for metallodrugs (Pt or non-Pt based) which (i) target the cell and/or (ii) have a different mode of action to Pt drugs currently in clinical use remains the subject of intense investigation [3].

Pt complexes having *trans* geometry [4], polynuclear Pt complexes [5] and Pt complexes with ligands capable of intercalating DNA [6] represent an emerging class of anti-tumour active compounds that circumvent some

* Corresponding author. Tel.: +353 01 4022161; fax: +353 01 4022168.
E-mail address: cmarmion@rcsi.ie (C.J. Marmion).

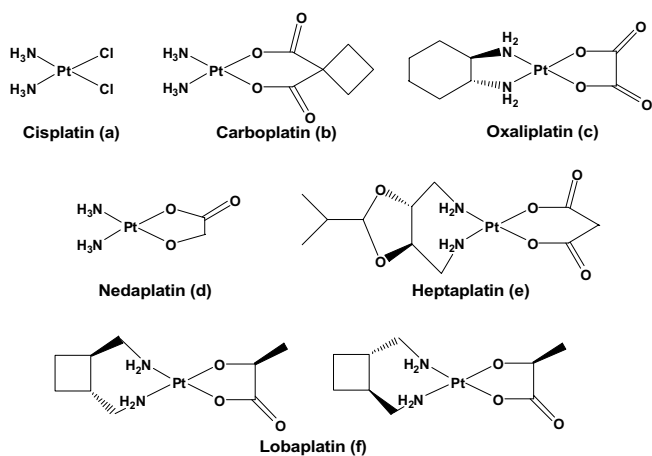


Fig. 1. Structures of cisplatin, carboplatin, oxaliplatin, nedaplatin, heptaplatin and lobaplatin.

of the problems associated with clinically used Pt drugs. They break the cisplatin paradigm by binding to DNA in other ways and may therefore be active against cisplatin-resistant cancer cell lines. Pt^{IV} complexes are also under investigation [7] where they are thought to be activated by reduction in the more reducing environment of cancer cells, thereby acting as prodrugs of the corresponding anti-tumour active Pt^{II} derivatives. An additional strategy to overcome the drawbacks associated with clinically used Pt drugs is to tether biologically-active ligands to the Pt which have, in themselves, inherent anti-tumour properties [1,3].

Nitric oxide (NO) has emerged as one of the most versatile and ubiquitous molecules in the human body with a diverse range of physiological functions including, amongst others, gene regulation, cytostasis, platelet function, vascular smooth muscle relaxation and proliferation, memory, immune stimulation and apoptosis [8–10]. It is derived from L-arginine *via* the catalytic action of a remarkable class of haem-containing metalloenzymes, the NO synthases (NOS), of which three different isoforms are known to exist; endothelial NOS (eNOS), neuronal NOS (nNOS) and inducible NOS (iNOS) [9,10].

Expression of NOS has been demonstrated in a variety of human and murine tumour types including gynecological, breast, head and neck, prostate, bladder and colon cancers and central nervous system tumours such as glioblastomas [11]. The toxic properties of NO are harnessed, within the immune system, in order to facilitate the control of infections and tumour cell growth [11,12]. Generated by iNOS, at high $\mu\text{mol/L}$ concentrations at the site of infection, NO is thought to attack cancer cells by binding to metal centres involved in their respiration, thereby disrupting their function [10,13]. Additionally, NO has been demonstrated to upregulate p53, the tumour suppressor gene [10]. NO-mediated inhibition of DNA synthesis may also be an important mechanism by which macrophages induce cytotoxicity. NO can induce DNA

damage by generating reactive nitrogen oxide species (RNOS) such as peroxyxynitrite and ONOO^- , which can oxidise and nitrate DNA and potentially cause single-strand DNA breaks *via* attack on the sugar–phosphate backbone [10,14]. Dinitrogen trioxide, another RNOS derived from NO, can nitrosate amines to form carcinogenic *N*-nitrosamines, which can then alkylate DNA [10,15].

Conflicting reports of pro- and anti-cancer activity associated with NO clearly illustrate the need for further research in this area in order to fully elucidate and understand the precise role of NO in cancer biology. High concentrations of NO, for example, can promote tumour cell death by apoptosis whereas lower concentrations of NO can promote tumour cell proliferation, vascularisation or even resistance to apoptosis [10,11]. In addition to concentration, the cellular effects of NO also depend on its source, latency, cell type and phenotype [10].

NO donors are currently under investigation as therapeutic agents for the treatment of a variety of disease states including cancer [16,17]. We recently reported that hydroxamic acids (RC(O)NHOH), a class of organic bioligands with a diverse range of biological functions [18,19], can act as effective NO donors by virtue of the fact that they readily transfer NO to ruthenium(III) (Ru^{III}) to form stable Ru^{II} nitrosyls. Moreover, in recent years, although there has been a surge of interest in developing novel Ru^{II} nitrosyl complexes, capable of releasing cytotoxic NO [20–23], as yet there is little or no evidence in the literature of NO-releasing Pt-based chemotherapeutics. The potential of NO delivery systems in the enhancement of platinum cytotoxicity has however been demonstrated, by pretreating Chinese hamster V79 lung fibroblast cells with bolus NO or NO delivered from NONOate NO donors. The tumour cells were markedly sensitized to subsequent cisplatin treatment [24]. It was on this premise that we wished to employ a novel synergistic approach, exploiting the well-established anti-cancer properties of Pt and the NO-releasing ability of hydroxamic acids and, in so doing, advance a new class of bifunctional metallodrug with dual DNA-binding and NO-releasing properties. 3- and 4-pyridinehydroxamic acids were specifically chosen with a view to synthesising Pt pyridinehydroxamic acid complexes where the pyridine nitrogen would selectively coordinate Pt^{II} or Pt^{IV} thereby leaving the hydroxamic acid moiety uncoordinated and potentially free to release cytotoxic NO.

Herein, we describe the synthesis, characterisation and NO-releasing ability of a novel class of 3- and 4-pyridinehydroxamic acid (3- and 4-pyhaH) complexes of Pt^{II} and Pt^{IV} . The crystal structure of the Pt^{IV} derivative, *cis*- $[\text{PtCl}_4(4\text{-pyhaH})_2] \cdot 2\text{CH}_3\text{OH}$ is reported. The corresponding 3- and 4-pyridinecarboxylic acid (3- and 4-pycaH) Pt^{II} and Pt^{IV} complexes, together with the Pt^{II} pyridine analogue were also synthesised and characterised to serve as reference standards in biological testing.

2. Experimental

2.1. General

3-Pyridinecarboxylic acid (nicotinic acid) **3**, 4-pyridinecarboxylic acid (isonicotinic acid) **4**, benzohydroxamic acid **5**, methylnicotinate, ethylisonicotinate and pyridine, were all purchased from Aldrich and used without further purification. $\text{K}_2[\text{Pt}^{\text{II}}\text{Cl}_4]$ and $\text{K}_2[\text{Pt}^{\text{IV}}\text{Cl}_6]$ were used as received from Johnson Matthey. $\text{K}[\text{Ru}^{\text{III}}(\text{Hedta})\text{Cl}]\cdot 2\text{H}_2\text{O}$ was synthesised as previously reported [25].

IR and far-IR spectroscopic measurements were obtained using a Mattson Genesis II CSI FTIR spectrometer. The spectra were analysed using WINFIRST software. Between 4000 and 400 cm^{-1} , KBr discs were employed while between 600 and 200 cm^{-1} , polythene discs (Nujol mull) were used. FTIR grade KBr and nujol were purchased from Aldrich. ^1H NMR spectra were recorded on a Bruker Avance 400 NMR spectrometer and the spectra analysed using TopSpin 1 software. Chemical shifts were measured relative to the undeuterated solvent peak. Elemental analysis was performed by the Microanalytical Laboratory, School of Chemistry & Chemical Biology, University College Dublin, Belfield, Dublin. Electrospray ionisation mass spectroscopy (ESI-MS) experiments were performed on a Quattro Micro quadrupole electrospray mass spectrometer (Micromass, Waters Corp., USA): 10 μL of the samples was injected in 300 μL of acetonitrile:water (60:40, v/v).

2.1.1. Synthesis of 3-pyridinehydroxamic acid (3-pyhaH) (1)

Hydroxylamine hydrochloride (5.1 g, 72 mmol) was added to sodium hydroxide (5.8 g, 146 mmol) in deionised water (37 ml). The resulting solution was then added dropwise to methylnicotinate (5.0 g, 36 mmol) in methanol (55 ml). The solution was stirred at room temperature for 72 h, after which the solution was acidified to pH 5.5 using 5% HCl. The solvent was removed *in vacuo* yielding a yellow solid. Methanol (60 ml) was added and sodium chloride filtered. The solvent was removed *in vacuo* yielding a light pink solid, which was recrystallised from water. Yield: 3.0 g, 22 mmol, 66%. *Anal. Calc.* for $\text{C}_6\text{H}_6\text{N}_2\text{O}_2$: C, 52.17; H, 4.38; N, 20.28. Found: C, 52.11; H, 4.24; N, 20.14%. ^1H NMR (400 MHz, $[\text{d}_6]$ -DMSO, 25 °C): $\delta = 11.25$ (s, 1H, OH), 9.13 (s, 1H, NH), 8.77 (s, 1H, aromatic H), 8.55 (d, 1H, aromatic H), 7.93 (d, 1H, aromatic H), 7.33 (dd, 1H, aromatic H).

2.1.2. Synthesis of 4-pyridinehydroxamic acid (4-pyhaH) (2)

4-pyhaH was synthesised from ethylisonicotinate in line with the procedure for 3-pyhaH described in Section 2.1.1 above. Yield: 74%. *Anal. Calc.* for $\text{C}_6\text{H}_6\text{N}_2\text{O}_2$: C, 52.17; H, 4.38; N, 20.28. Found: C, 52.20; H, 4.26; N, 20.18%. ^1H NMR (400 MHz, $[\text{d}_6]$ -DMSO, 25 °C): $\delta = 11.42$ (s, 1H, OH), 9.25 (s, 1H, NH), 8.57 (dd, 2H, aromatic H), 7.54 (dd, 2H, aromatic H).

2.1.3. Synthesis of *cis*- $[\text{Pt}^{\text{II}}\text{Cl}_2(3\text{-pyhaH})_2]\cdot 2\text{H}_2\text{O}$ (6)

3-Pyridinehydroxamic acid (3-pyhaH) (0.146 g, 1.06 mmol) in methanol (7 ml) was added to $\text{K}_2[\text{Pt}^{\text{II}}\text{Cl}_4]$ (0.20 g, 0.48 mmol) in deionised water (7 ml). The resulting solution was stirred without protection from light at room temperature for 24 h turning yellow in colour. A yellow precipitate was filtered and dried over P_2O_5 . Yield: 0.18 g, 0.31 mmol, 65%. *Anal. Calc.* for $\text{PtC}_{12}\text{H}_{16}\text{N}_4\text{O}_6\text{Cl}_2$: C, 24.92; H, 2.79; N, 9.69; Cl, 12.26. Found: C, 24.88; H, 2.65; N, 9.64; Cl, 12.35%. ^1H NMR (400 MHz, $[\text{d}_6]$ -DMSO, 25 °C): $\delta = 11.48$ (s, 2H, OH), 9.31 (s, 2H, NH), 8.98 (s, 2H, aromatic H), 8.76 (d, 2H, aromatic H), 8.14 (d, 2H, aromatic H), 7.47 (dd, 2H, aromatic H).

The Pt^{II} and Pt^{IV} compounds, **7–14**, were synthesised by reaction of the appropriate pyridine derivative or pyridine with either $\text{K}_2[\text{Pt}^{\text{II}}\text{Cl}_4]$ or $\text{K}_2[\text{Pt}^{\text{IV}}\text{Cl}_6]$, respectively, by the method described in Section 2.1.3 above.

2.1.4. *cis*- $[\text{Pt}^{\text{II}}\text{Cl}_2(4\text{-pyhaH})_2]\cdot \text{H}_2\text{O}$ (7)

Yield: 70%. *Anal. Calc.* for $\text{PtC}_{12}\text{H}_{14}\text{N}_4\text{O}_5\text{Cl}_2$: C, 25.73; H, 2.52; N, 10.00; Cl, 12.66. Found: C, 25.94; H, 2.34; N, 9.74; Cl, 12.49%. ^1H NMR (400 MHz, $[\text{d}_6]$ -DMSO, 25 °C): $\delta = 11.53$ (s, 2H, OH), 9.43 (s, 2H, NH), 8.78 (dd, 4H, aromatic H), 7.59 (dd, 4H, aromatic H).

2.1.5. *cis*- $[\text{Pt}^{\text{II}}\text{Cl}_2(3\text{-pycaH})_2]$ (8)

Yield: 69%. *Anal. Calc.* for $\text{PtC}_{12}\text{H}_{10}\text{N}_2\text{O}_4\text{Cl}_2$: C, 28.14; H, 1.97; N, 5.47; Cl, 13.84. Found: C, 28.01; H, 1.90; N, 5.25; Cl, 13.56%. ^1H NMR (400 MHz, $[\text{d}_6]$ -DMSO, 25 °C): $\delta = 9.19$ (s, 2H, aromatic H), 8.84 (d, 2H, aromatic H), 8.33 (d, 2H, aromatic H), 7.45 (dd, 2H, aromatic H).

2.1.6. *cis*- $[\text{Pt}^{\text{II}}\text{Cl}_2(4\text{-pycaH})_2]$ (9)

Yield: 77%. *Anal. Calc.* for $\text{PtC}_{12}\text{H}_{10}\text{N}_2\text{O}_4\text{Cl}_2$: C, 28.14; H, 1.97; N, 5.47; Cl, 13.84. Found: C, 28.11; H, 1.91; N, 5.27; Cl, 13.96%. ^1H NMR (400 MHz, $[\text{d}_6]$ -DMSO, 25 °C): $\delta = 8.79$ (dd, 4H, aromatic H), 7.70 (dd, 4H, aromatic H).

2.1.7. *cis*- $[\text{Pt}^{\text{II}}\text{Cl}_2(\text{py})_2]$ (10)

Yield: 75%. *Anal. Calc.* for $\text{PtC}_{10}\text{H}_{10}\text{N}_2\text{Cl}_2$: C, 28.31; H, 2.38; N, 6.60. Found: C, 28.21; H, 2.15; N, 6.38%. ^1H NMR (400 MHz, $[\text{d}_6]$ -DMSO, 25 °C): $\delta = 8.47$ (d, 4H, aromatic H), 7.49 (t, 4H, aromatic H), 7.32 (m, 2H, aromatic H).

2.1.8. *cis*- $[\text{Pt}^{\text{IV}}\text{Cl}_4(3\text{-pyhaH})_2]\cdot 2\text{H}_2\text{O}$ (11)

Yield: 63%. *Anal. Calc.* for $\text{PtC}_{12}\text{H}_{16}\text{N}_4\text{O}_6\text{Cl}_4$: C, 22.20; H, 2.48; N, 8.63; Cl, 21.85. Found: C, 22.47; H, 2.41; N, 8.48; Cl, 21.69%. ^1H NMR (400 MHz, $[\text{d}_6]$ -DMSO, 25 °C): $\delta = 11.79$ (s, 2H, OH), 9.51 (s, 2H, NH), 9.13 (s, 2H, aromatic H), 8.88 (d, 2H, aromatic H), 8.26 (d, 2H, aromatic H), 7.48 (dd, 2H, aromatic H).

2.1.9. *cis*- $[\text{Pt}^{\text{IV}}\text{Cl}_4(4\text{-pyhaH})_2]\cdot 2\text{CH}_3\text{OH}$ (12)

Yield: 63%. *Anal. Calc.* for $\text{PtC}_{14}\text{H}_{20}\text{N}_4\text{O}_6\text{Cl}_4$: C, 24.83; H, 2.98; N, 8.27; Cl, 20.94. Found: C, 24.77; H, 2.91; N,

8.22; Cl, 20.78%. ^1H NMR (400 MHz, $[d_6]$ -DMSO, 25 °C): $\delta = 11.88$ (s, 2H, OH), 9.64 (s, 2H, NH), 8.85 (dd, 4H, aromatic H), 7.97 (dd, 4H, aromatic H).

2.1.10. *cis*-[Pt^{IV}Cl₄(3-pycaH)₂] (13)

Yield: 61%. *Anal.* Calc. for PtC₁₂H₁₀N₂O₄Cl₄: C, 24.72; H, 1.73; N, 4.80; Cl, 24.32. Found: C, 24.70; H, 1.69; N, 4.63; Cl, 24.11%. ^1H NMR (400 MHz, $[d_6]$ -DMSO, 25 °C): $\delta = 9.23$ (s, 2H, aromatic H), 8.61 (m, 4H, aromatic H), 7.66 (dd, 2H, aromatic H).

2.1.11. *cis*-[Pt^{IV}Cl₄(4-pycaH)₂] (14)

Yield: 67%. *Anal.* Calc. for PtC₁₂H₁₀N₂O₄Cl₄: C, 24.72; H, 1.73; N, 4.80; Cl, 24.32. Found: C, 24.56; H, 1.91; N, 4.55; Cl, 24.17%. ^1H NMR (400 MHz, $[d_6]$ -DMSO, 25 °C): $\delta = 8.79$ (dd, 4H, aromatic H), 7.98 (dd, 4H, aromatic H).

2.1.12. K[Ru^{II}(Hedta)(NO)Cl] · H₂O (15)

cis-[Pt^{II}Cl₂(3-pyhaH)₂] · 2H₂O (6) (0.29 g, 0.50 mmol) was added to a yellow aqueous solution (15 ml) of K[Ru^{III}(Hedta)Cl] · 2H₂O (0.25 g, 0.50 mmol), resulting in a reddish solution. The reaction was refluxed for 3 h whereupon it turned brown in colour. The reaction was concentrated in vacuo (~5 ml), purified on a sephadex column LH20 using water as eluent to give K[Ru(Hedta)(NO)Cl] · H₂O as a brown solid. Yield: 58%. *Anal.* Calc. for RuC₁₀H₁₅N₃ClKO₁₀: C, 23.42; H, 2.95; N, 8.19; Cl, 6.91; K, 7.62. Found: C, 23.45; H, 2.91; N, 8.42; Cl, 6.97; K, 7.46%. ^1H NMR (400 MHz, D₂O, 25 °C): $\delta = 4.43$ (d, 2H, CH₂ glycine), 4.34 (s, 2H, CH₂ glycine), 4.09 (2H, s, CH₂ glycine), 3.84 (2H, s, CH₂ glycine) 3.61 (4H, m, CH₂ ethylenediamine); ^{13}C NMR (400 MHz; D₂O; 25 °C): $\delta = 181.8, 178.5$ (CO bound glycinate), 177.7, 168.8 (CO free glycinate), 65.45, 65.4, 64.7, 64.3 (CH₂ glycinate), 62.8, 60.4 (CH₂ ethylenediamine); $\nu_{\text{max}}/\text{cm}^{-1}$ 3345s (OH), 2986s, 2947s (CH, H₂edta), 1894vs (NO), 1726s (CO free glycine arms) and 1649b (CO bound glycine arms); ESI-MS *m/z*: 456 ([M–H][−]).

K[Ru^{II}(Hedta)(NO)Cl] · H₂O (15) was likewise obtained by reacting *cis*-[Pt^{II}Cl₂(4-pyhaH)₂] · H₂O (7) with K[Ru^{III}(Hedta)Cl] · 2H₂O in line with the procedure described above.

2.2. Structural characterisation of *cis*-[Pt^{IV}Cl₄(4-pyhaH)₂] · 2CH₃OH (12)

Crystal data and experimental details for **12** are summarised in Table 1. The structure of **12** was refined in the *Pbcn* space group. Crystal data were collected on a Bruker Smart Apex CCD diffractometer at 100 K using monochromated Mo K α radiation, ($\lambda = 0.71073$ Å) and the $\phi - \omega$ scan method. The structure was solved by direct method (SHELXS-97) [26] and refined by full-matrix least squares using SHELXL 97-2 package [26]. All hydrogen atoms were localised in the difference fourier map and allowed to refine freely.

Table 1
Summary of crystal data for **12**

Empirical formula	C ₁₄ H ₂₀ N ₄ O ₆ Cl ₄ Pt
Formula weight	677.23
Temperature (K)	100(2)
Wavelength (Å)	0.71073
Crystal system	orthorhombic
Space group	<i>Pbcn</i>
<i>Unit cell parameters</i>	
<i>a</i> (Å)	7.3794(5)
<i>b</i> (Å)	11.9791(8)
<i>c</i> (Å)	24.8071(17)
α (°)	90
β (°)	90
γ (°)	90
Volume (Å ³), <i>Z</i>	2192.9(3), 4
<i>D</i> _{calc} (Mg/m ³)	2.051
Absorption coefficient (mm ^{−1})	6.924
<i>F</i> (000)	1304
Crystal size (mm)	0.30 × 0.20 × 0.20
θ Range for data (°)	3.21–29.46
Index ranges	−9 ≤ <i>h</i> ≤ 9, −16 ≤ <i>k</i> ≤ 16, −33 ≤ <i>l</i> ≤ 32
Reflections collected	18484
Independent reflections (<i>R</i> _{int})	2891 (0.0289)
Completeness to $\theta = 29.46^\circ$ (%)	94.8
Absorption correction	semi-empirical from equivalents
Maximum and minimum transmission	0.3381 and 0.2305
Refinement method	full-matrix least-squares on <i>F</i> ²
Data/restraints/parameters	2891/0/172
Goodness-of-fit on <i>F</i> ²	1.049
Final <i>R</i> indices [<i>I</i> > 2 σ (<i>I</i>)]	<i>R</i> ₁ = 0.0217, <i>wR</i> ₂ = 0.0453
<i>R</i> indices (all data)	<i>R</i> ₁ = 0.0277, <i>wR</i> ₂ = 0.0471
Largest difference in peak and hole (e Å ^{−3})	1.713 and −0.904

$$R_1 = \frac{\sum |F_o| - |F_c|}{\sum |F_o|}, wR_2 = \frac{[\sum w(F_o^2 - F_c^2)^2 / \sum w(F_o^2)^2]^{1/2}}$$

2.3. Pharmacological tests

The NO-releasing properties of the test compounds were investigated using an isolated organ bath experiment as follows. Thoracic aorta rings were prepared from male Wistar Hannover rats weighing about 250–400 g purchased from the animal facility of the University of Trieste. The animals were maintained according to the guidelines in force in Italy (DDL 116, 21/02/92 and subsequent addenda) and in compliance with the “Guide for the care and use of laboratory animals” DHIIS Publ. No (NHI) 86-23, Bethesda, MD, NHI (1985). Rat thoracic aortas were carefully removed, after killing of the animals by CO₂ overdose, put into a Petri dish containing Krebs solution (containing 118.3 mM NaCl, 25 mM NaHCO₃, 4.8 mM KCl, 2.5 mM CaCl₂, 1.2 mM MgSO₄, 1.2 mM KH₂PO₄, 11.1 mM glucose, at pH 7.4), and cleaned of fat and of connective tissue. Aorta rings, cut at about 2 mm, were put into a 20 mL organ bath (model 4050, Ugo Basile, Padova Italy) with constant gas flow (95% O₂ + 5% CO₂) at 37 ± 0.5 °C. Two stainless steel hooks were inserted into the aortic lumen to fix the test sample to the bath bottom and to connect it to a force transducer. Aortic rings were equilibrated with Krebs solution and maintained under an optimal ten-

sion of 2 g for 40 min before experiments. Rings were stimulated with 30 mM KCl to assess the integrity of the strips (rings with abnormal contraction were discarded), and responsive rings were rinsed with Krebs solution and allowed to equilibrate for a further 30 min. Contraction was elicited by adding phenylephrine (dissolved in ultrapure water) to the bath (final concentration 3×10^{-7} M). Once sample contraction reached a plateau, the relaxation–response curve was obtained by cumulative additions of acetylcholine (dissolved in ultrapure water) to the organ bath (final concentrations ranging between 10^{-9} M and 10^{-4} M). After their maximal relaxation, aorta rings were rinsed with Krebs solution and allowed to re-equilibrate for 30 min. Contraction was elicited again by phenylephrine, and compounds **1–10** were tested in the concentration interval between 10^{-9} and 10^{-4} M (stock solutions were prepared in DMSO with subsequent dilutions in ultra-pure water in order to keep DMSO in the bath to less than 0.1%); cisplatin was used as control, at the same concentrations and conditions.

The vehicle used for dissolving the test complexes was also tested for relaxation. Contraction or relaxation were recorded isometrically *via* a force–displacement transducer (model 7003, Ugo Basile, Padova, Italy) connected to a Unirecord Microdynamometer recorder (model 7050, Ugo Basile, Padova, Italy). Experiments with compounds **6** and **8** were repeated in the presence of 10 μ M methylene blue (dissolved in ultrapure water), a guanylate cyclase inhibitor [27]. In this case, methylene blue was added to the organ bath, for 10 min, every time before inducing contraction with phenylephrine. For each compound, experiments were replicated at least three times.

2.4. Statistical analysis

Data were submitted to computer-assisted statistical analysis using ANOVA analysis of variance and Tukey–Kramer multiple comparison post-test or Student *t*-test.

3. Results and discussion

3.1. Synthesis and spectroscopic characterisation of ligands 1–4

3- and 4-pyridinecarboxylic acid (3- and 4-pycaH) were used as purchased and a selection of IR spectral data are provided in [Supplementary data](#).

The hydroxamic acids were synthesised by reacting the corresponding carboxylic methyl or ethylesters with hydroxylamine in aqueous methanol in line with literature methods [28]. They were obtained in good yields (55–85%) and excellent purity and were characterised by elemental analysis, IR and ^1H NMR spectroscopy. The IR spectra of 3-pyhaH **1** and 4-pyhaH **2** contain stretches between $3180\text{--}3190\text{ cm}^{-1}$, $2800\text{--}2850\text{ cm}^{-1}$ and $1640\text{--}1660\text{ cm}^{-1}$ which may be assigned to $\nu_{\text{O-H}}$, $\nu_{\text{N-H}}$ and $\nu_{\text{C=O}}$, respectively. The symmetric and asymmetric stretches corre-

sponding to $\nu_{\text{C=O}}$ are found as only one stretch due to intramolecular hydrogen bonding, while the broad $\nu_{\text{O-H}}$ of the hydroxamato may be attributed to intermolecular hydrogen bonding. These values concur with those previously reported in the literature [29,30]. Selected IR spectral data for **1** and **2** are provided in [Supplementary data](#).

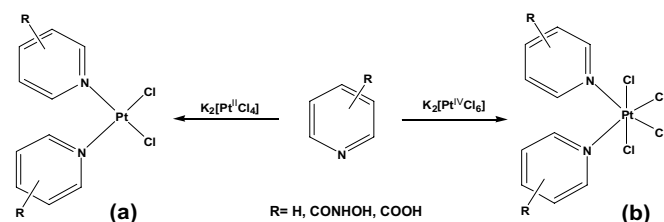
The ^1H NMR spectra of the hydroxamic acids **1** and **2** in d_6 -DMSO show N–H and O–H resonances at *ca.* 9.2 ppm and 11.3 ppm, respectively, both of which are concentration-dependent due to extensive intermolecular hydrogen bonding at high concentrations. The ^1H NMR spectrum of **1** exhibits 4 resonances at 8.77, 8.55, 7.93 and 7.33 ppm corresponding to the four protons of the *meta*-substituted pyridine ring, while that of **2** has two resonances at 8.57 and 7.54 ppm corresponding to the four protons of the *para*-substituted derivative.

3.2. Synthesis and characterisation of Pt^{II} and Pt^{IV} complexes 6–14

The dichlorido Pt^{II} complexes, **6–10** and their Pt^{IV} analogues, **11–14** were prepared by reaction of $\text{K}_2[\text{Pt}^{\text{II}}\text{Cl}_4]$ or $\text{K}_2[\text{Pt}^{\text{IV}}\text{Cl}_6]$, respectively, with the appropriate pyridine derivative (pyd) in aqueous or aqueous/methanolic solutions ([Scheme 1](#)).

The previously reported Pt^{II} pyridine analogue, *cis*- $[\text{Pt}^{\text{II}}\text{Cl}_2(\text{py})_2]$ **10** [31], was also synthesised to serve as a reference standard in biological testing. In all cases the yellow Pt^{II} and Pt^{IV} products were obtained in good yield (60–80%) and excellent purity and were further characterised by IR and ^1H NMR spectroscopy. The *cis*-configurations of the Pt^{II} complexes, **6–10** ([Fig. 2](#)), were confirmed by the classic Kurnakov test [32].

The spectroscopic data for the Pt^{II} and Pt^{IV} pyhaH and pycaH complexes are consistent with coordination *via* the pyridine nitrogen and reveal the free nature of the uncoordinated hydroxamic or carboxylic acid moiety as expected. Selected IR and far-IR spectral data for the free ligands and Pt^{II} and Pt^{IV} complexes are provided in [Supplementary data](#) ([Table 1](#)). Briefly the $\nu_{\text{C=O}}$ of the Pt pyhaH and pycaH complexes are found at *ca.* 1660 and 1705 cm^{-1} , respectively, and as expected are comparable to those of the corresponding free ligands. The hydroxamic acid complexes, in addition, display sharp $\nu_{\text{N-H}}$ and broad $\nu_{\text{O-H}}$ stretches, again comparable to those of the corresponding free ligands. Far-IR data can also be particularly useful in determining the stereochemistry of the complexes



Scheme 1. Synthesis of (a) *cis*- $[\text{Pt}^{\text{II}}\text{Cl}_2(\text{pyd})_2]$ and (b) *cis*- $[\text{Pt}^{\text{IV}}\text{Cl}_4(\text{pyd})_2]$.

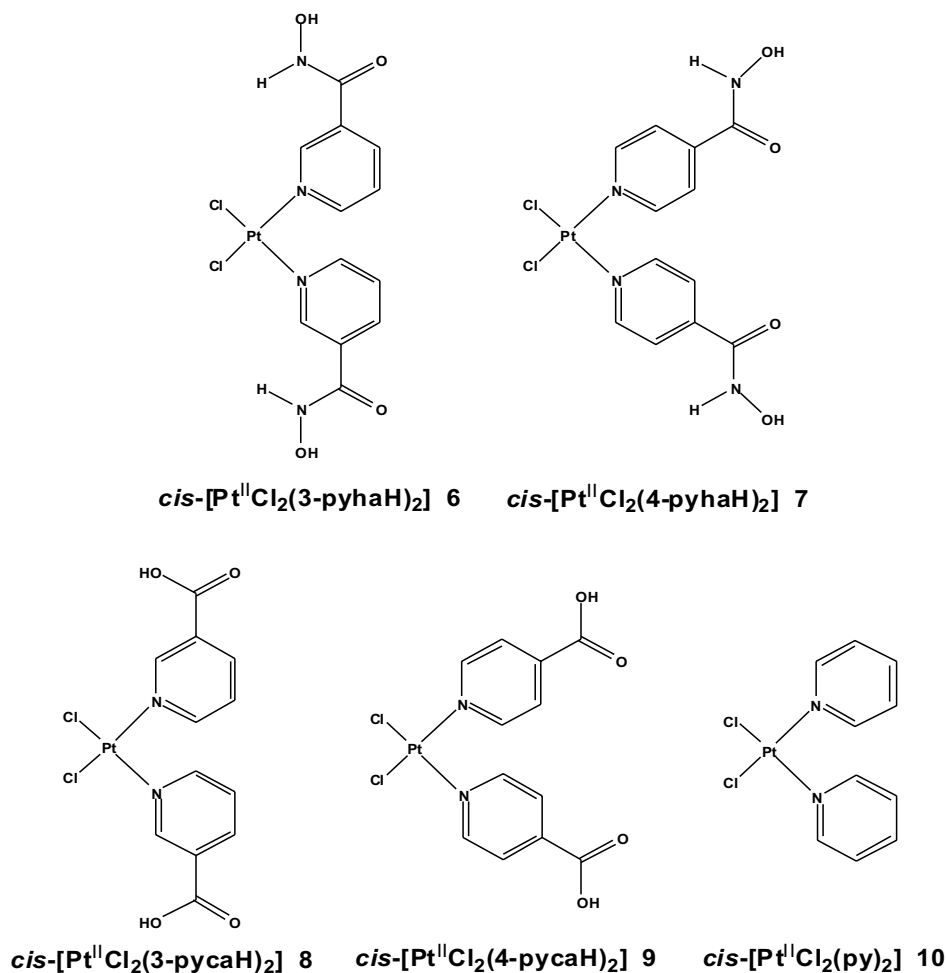


Fig. 2. Structures of the dichlorido Pt^{II} complexes.

synthesised. For a square planar Pt^{II} complex of general formula PtCl₂L₂, where L is a monodentate ligand, the *trans*-isomer (*D*_{2h}) exhibits only one $\nu_{\text{Pt-Cl}}$ whereas the *cis*-isomer (*C*_{2v}) exhibits two stretches. For Pt^{IV} complexes of type PtCl₄L₂, the *trans*-isomer (*D*_{4h}) exhibits one $\nu_{\text{Pt-Cl}}$ and the *cis*-isomer (*C*_{2v}) exhibits four [33]. The far-IR data support the *cis* configuration for **6** and **8–14**. Occasionally the $\nu_{\text{Pt-Cl}}$ merge as is the case with *cis*-[Pt^{II}Cl₂(4-pyhaH)₂] **7** and the configuration of the complex cannot be accurately determined from far-IR data alone.

The ¹H NMR spectra for all the Pt complexes support the presence of one isomer only. For the pyhaH complexes **6**, **7**, **11** and **12** in *d*⁶-DMSO, N–H and O–H resonances are observed at *ca.* 9.3 ppm and *ca.* 11.5 ppm, respectively, and are, as expected, comparable to those of the free ligands. The ¹H NMR spectrum of *cis*-[Pt^{II}Cl₂(3-pyhaH)₂] contains 4 resonances at 8.98, 8.76, 8.14 and 7.47 ppm corresponding to the eight protons of the *meta*-substituted pyridine rings. A similar overall pattern is observed in the ¹H NMR spectra of the Pt^{II} and Pt^{IV} complexes with 4 and 2 resonances integrating well for the complexes with coordinated *meta* and *para*-substituted pyridine rings, respectively, and a shift consistent with complexation.

3.3. Structural characterisation of *cis*-[Pt^{IV}Cl₄(4-pyhaH)₂] · 2CH₃OH (**12**)

Yellow crystals of **12** suitable for a single crystal X-ray diffraction experiment were obtained by slow evaporation from a methanol solution. The atomic numbering scheme and atom connectivity for **12** are shown in Fig. 3 and a selection of bond lengths and angles reported in Table 2. In **12**, the Pt^{IV} complex displays a near perfect octahedral geometry, not surprisingly given its symmetric nature. The N(1)–Pt–N(1) and the Cl(2)#1–Pt–Cl(2) bond angles are 178.42(6)° and 179.86(4)°, respectively. The N(1)–Pt–Cl(1)#1 and N(1)–Pt–Cl(2)#1 bond angles are 89.91(6)° and 89.21(7)°, respectively. The Pt–Cl bond lengths range from 2.295(1) to 2.308(1) Å and the shorter Pt–N bond lengths are 2.062(2) Å. The two pyhaH ligands lie in the *cis*-configuration where each is present as a monodentate ligand coordinated *via* the pyridine nitrogen only with an uncoordinated hydroxamic acid functional group.

In addition, hydroxamic acids are known to adopt one of two tautomeric forms, the enol and the keto, each of which can exist as *E* or *Z* conformers [19], where the stereodescriptors *E* and *Z* are used to describe the *trans* and *cis*

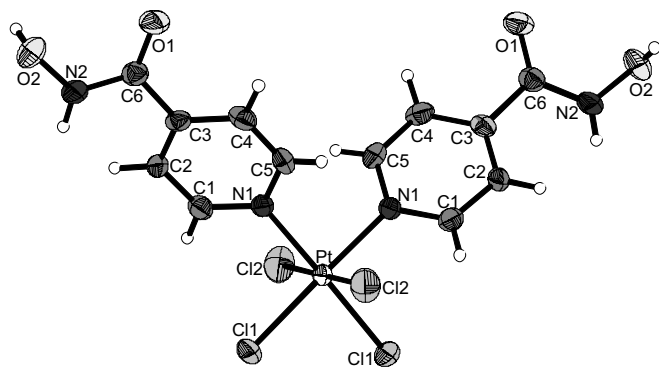


Fig. 3. ORTEP diagram of **12** with solvent molecules omitted. The atomic numbering scheme is displayed (thermal ellipsoids at 80% probability level).

Table 2
Selected bond lengths (Å) and angles (°) with estimated standard deviations for **12**

Bond atoms	Distance (Å)	Angle atoms	Angle (°)
Pt–N(1)	2.062(2)	N(1)–Pt–N(1)#1	91.66(12)
Pt–N(1)#1	2.062(2)	N(1)–Pt–Cl(1)#1	89.91(6)
Pt–Cl(1)#1	2.2951(7)	N(1)#1–Pt–Cl(1)#1	178.42(6)
Pt–Cl(1)	2.2951(7)	N(1)–Pt–Cl(1)	178.42(6)
Pt–Cl(2)#1	2.3084(7)	N(1)#1–Pt–Cl(1)	89.91(6)
Pt–Cl(2)	2.3084(7)	Cl(1)#1–Pt–Cl(1)	88.51(4)
C(3)–C(6)	1.497(3)	N(1)–Pt–Cl(2)#1	89.21(7)
C(6)–O(1)	1.232(3)	N(1)#1–Pt–Cl(2)#1	90.69(7)
C(6)–N(2)	1.330(3)	Cl(1)#1–Pt–Cl(2)#1	89.18(3)
N(2)–O(2)	1.394(3)	Cl(1)–Pt–Cl(2)#1	90.93(3)
		N(1)–Pt–Cl(2)	90.69(7)
		N(1)#1–Pt–Cl(2)	89.21(7)
		Cl(1)#1–Pt–Cl(2)	90.93(3)
		Cl(1)–Pt–Cl(2)	89.18(3)
		Cl(2)#1–Pt–Cl(2)	179.86(4)

orientation of the OH and C=O groups of the hydroxamic acid. The X-ray structural determination of **12** evidenced the free hydroxamic acid moieties in the keto form, adopt-

ing *Z* conformation. The hydroxamic acid NH and OH each hydrogen-bond to the oxygen acceptor atoms of different methanol solvent molecules with NH···O and OH···O bond length of approximately 2.00 and 1.81 Å, respectively, while the hydroxamic acid carbonyl oxygen hydrogen-bonds to a third methanol solvent molecule with an O···HO bond length of approximately 1.86 Å (Supplementary data, Fig. 1 and Table 2). With the complex situated on a twofold axis, a three-dimensional hydrogen-bonded lattice results (Fig. 4). The hydrogen-bond distances and angles are presented in Supplementary data (Table 2).

The crystal structure of **12**, together with a comparison of the far-IR spectral data for **12** with those of **11**, **13** and **14**, assist in the definitive assignment of the *cis*-configuration for each of the Pt^{IV} pyhaH and pycaH complexes synthesised (Fig. 5). Selected IR and far-IR spectral data are provided in Supplementary data (Table 1).

3.4. Synthesis and characterisation of $K[Ru^{II}(Hedta)(NO)Cl] \cdot H_2O$ (**15**)

To establish that the free hydroxamic acid moieties in *cis*-[Pt^{II}Cl₂(*x*-pyhaH)₂] (*x* = 3, 4) are sources of NO, we reacted *cis*-[Pt^{II}Cl₂(*x*-pyhaH)₂] with the well-known ruthenium (Ru) NO scavenger, K[Ru^{III}(Hedta)Cl]·2H₂O, which resulted in the facile formation of the Ru^{II}-nitrosyl, K[Ru^{II}(Hedta)(NO)Cl]·H₂O. Reaction of *cis*-[PtCl₂(py)₂] with K[Ru^{III}(Hedta)Cl]·2H₂O did not yield a Ru^{II}-nitrosyl product.

The Ru^{II}-NO⁺ complex, K[Ru^{II}(Hedta)(NO)Cl]·H₂O (**15**) was obtained upon reaction of *cis*-[Pt^{II}Cl₂(*x*-pyhaH)₂] (*x* = 3, 4) i.e. **6** or **7** with the well-known NO scavenger, K[Ru^{III}(Hedta)Cl]·2H₂O. Elemental analysis, IR, ¹H and ¹³C NMR and ESI-mass spectra are consistent with the formulation, K[Ru^{II}(Hedta)(NO)Cl]·H₂O and concur with previously reported examples of Ru^{II}-edta-NO

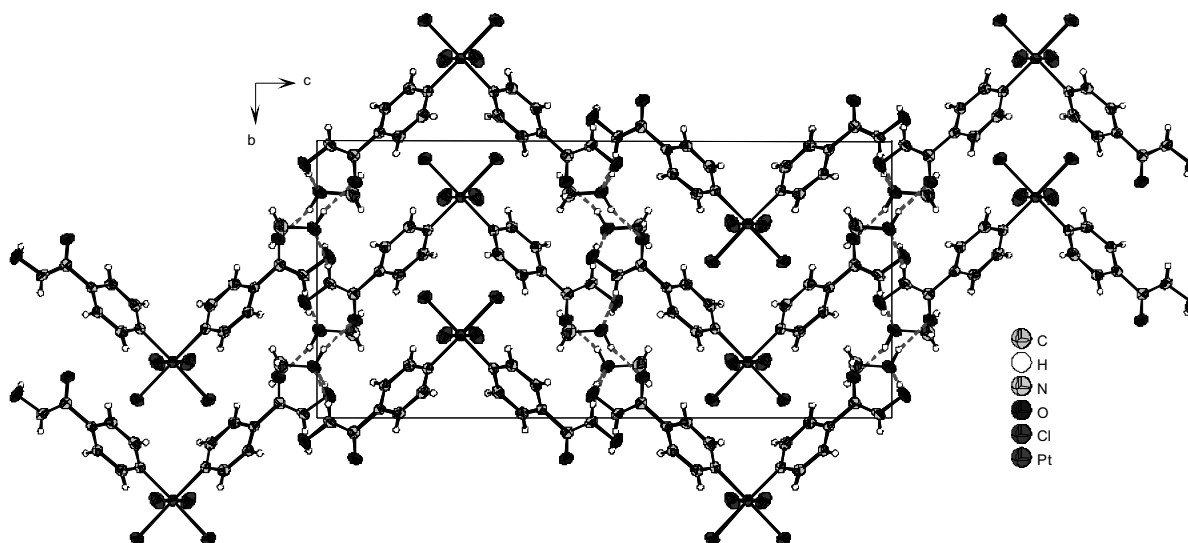


Fig. 4. Crystal packing of **12**. View of three-dimensional hydrogen-bonded lattice along [100] (thermal ellipsoids at 50% probability level).

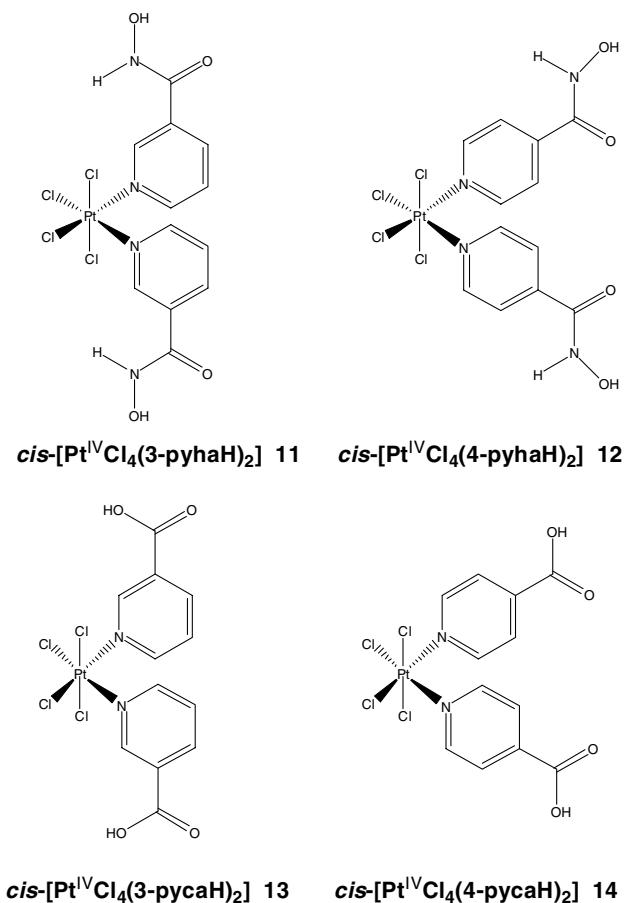


Fig. 5. Structures of tetrachlorido Pt^{IV} complexes.

complexes in the literature [34]. The IR spectra of **15** contains a distinctive ν_{NO} at 1894 cm^{-1} . ESI-MS in the negative mode was used to unequivocally identify the Ru^{II}-NO⁺ complex, [Ru^{II}(Hedta)(NO)Cl]⁻; a mass peak at 456 amu with the correct isotopic abundances was observed. Previous reported reactions of K[Ru^{III}(Hedta)Cl]·2H₂O with hydroxamic acids such as benzohydroxamic acid gave the Ru^{II}-NO⁺ complex, K₂[Ru^{II}(edta)(NO)Cl] [18]. The doubly protonated edta complex Ru(H₂edta)(NO)Cl was previously isolated by reacting K[Ru(Hedta)Cl]·2H₂O with *N*-methyl-*N*-nitroso-*p*-toluenesulfonamide or NO gas under argon [34]. Depending on pH, the Ru^{II}-NO⁺ complexes can be isolated with the free arm of the ethylenediaminetetraacetate in the protonated or the anionic form.

3.5. Pharmacological tests

The free ligands **1–4**, benzohydroxamic acid **5** and the Pt^{II} compounds **6–10** and their corresponding reference numbers are listed in Table 3.

The effects on vasorelaxation of Pt^{II} compounds **6–9**, the hydroxamic acid ligands **1** and **2**, the carboxylic acid ligands **3** and **4** and the control compounds, benzohydroxamic acid **5**, *cis*-[Pt^{II}Cl₂(py)₂] (**10**), and cisplatin were stud-

Table 3

The free ligands, benzohydroxamic acid and the Pt^{II} compounds and their corresponding reference numbers

3-Pyridinehydroxamic acid (3-pyhaH)	1
4-Pyridinehydroxamic acid (4-pyhaH)	2
3-Pyridinecarboxylic acid (nicotinic acid) (3-pycaH)	3
4-Pyridinecarboxylic acid (isonicotinic acid) (4-pycaH)	4
Benzohydroxamic acid (bhaH)	5
<i>cis</i> -[Pt ^{II} Cl ₂ (3-pyhaH) ₂]·2H ₂ O	6
<i>cis</i> -[Pt ^{II} Cl ₂ (4-pyhaH) ₂]·H ₂ O	7
<i>cis</i> -[Pt ^{II} Cl ₂ (3-pycaH) ₂]	8
<i>cis</i> -[Pt ^{II} Cl ₂ (4-pycaH) ₂]	9
<i>cis</i> -[Pt ^{II} Cl ₂ (py) ₂]	10

ied using thoracic aorta rings isolated from rats. Given the fact that Pt^{IV} compounds are thought to be activated by reduction to their corresponding Pt^{II} analogues, the NO-releasing properties of the Pt^{IV} compounds herein described were not investigated.

Compounds **6** and **7**, as well as their ligands **1** and **2**, induce the same extent (~80% at the highest concentration used) of vasorelaxation of aortic rings pre-contracted with phenylephrine, irrespective of the position in the pyridine ring of the hydroxamic acid moiety (Fig. 6). Benzohydroxamic acid, used as a positive control [18], induces vasorelaxation to a lesser extent (Fig. 8). Ligands characterised by the presence of a carboxylic acid group, i.e. compounds **3** and **4**, induce mild relaxation of aorta rings, comparable to that induced by water (the solvent used to dissolve these compounds), that reaches approximately 30% at concentrations $\geq 10^{-7}\text{ M}$ (Fig. 7). In contrast, the corresponding Pt derivatives **8** and **9** cause vasorelaxation statistically (**3** versus **8** $p < 0.02$ for concentrations $\geq 10^{-7}\text{ M}$) greater than that of the free ligands, with a maximum of approximately 60%, at the highest concentration used (Fig. 7).

Cisplatin and *cis*-[Pt^{II}Cl₂(py)₂] **10**, studied in the same experimental model (Fig. 8), do not induce relaxation of the aorta rings (relaxation comparable to that induced by

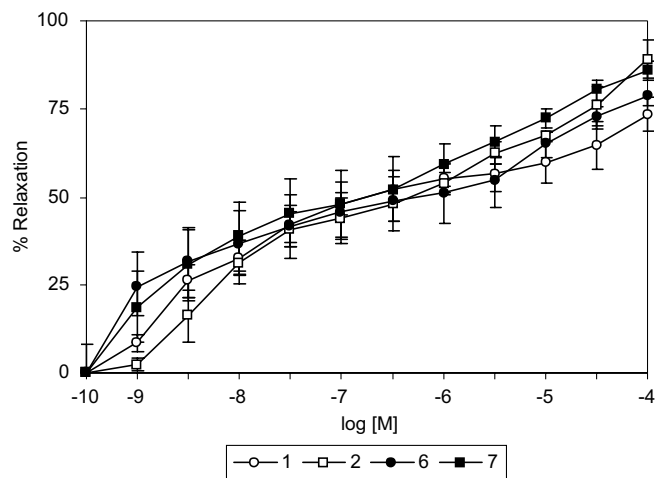


Fig. 6. Effects of compounds 3-pyhaH **1**, 4-pyhaH **2** and of respective platinum compounds *cis*-[Pt^{II}Cl₂(3-pyhaH)₂] (**6**) and *cis*-[Pt^{II}Cl₂(4-pyhaH)₂] (**7**) on aortic ring relaxation.

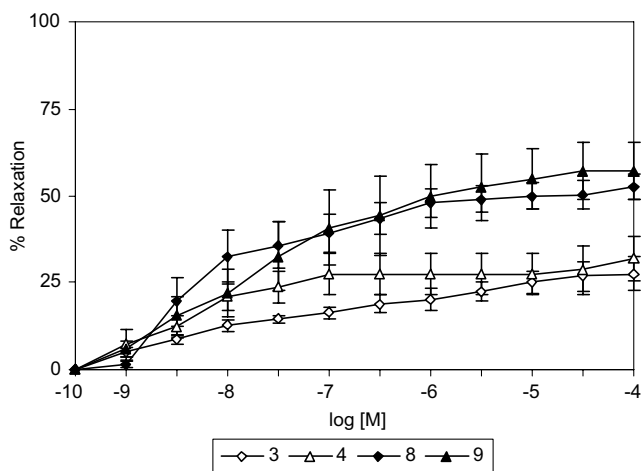


Fig. 7. Effects of compounds 3-pycaH **3**, 4-pycaH **4** and of respective platinum compounds *cis*-[Pt^{II}Cl₂(3-pycaH)₂] (**8**) and *cis*-[Pt^{II}Cl₂(4-pycaH)₂] (**9**) on aortic rings relaxation.

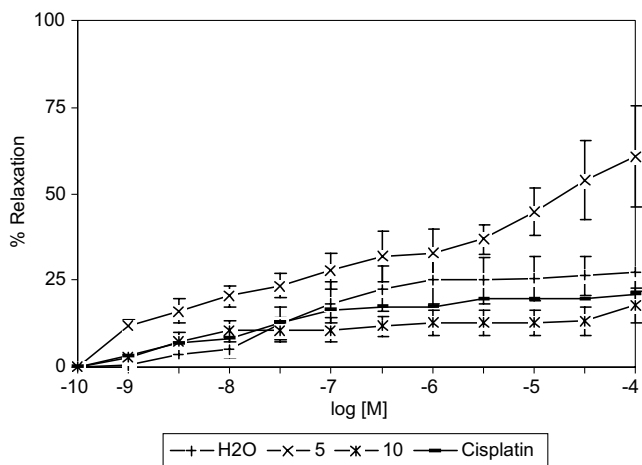


Fig. 8. Effects of water, benzohydroxamic acid **5**, *cis*-[Pt^{II}Cl₂(py)₂] (**10**) and cisplatin on aortic rings relaxation.

water) suggesting the lack of any role of the Pt ion *per se* in this phenomenon.

The involvement of NO in the induced vasorelaxation of compounds **6** and **8** was further investigated in the presence and absence of the guanylate cyclase inhibitor methylene blue (Fig. 9). Methylene blue completely abolished the vasorelaxation induced by both compounds **6** and **8**, indicating the involvement of the NO signaling pathway, likewise in the case of compound **8**, a derivative free of the hydroxamic acid moiety.

This data show that both hydroxamic acid and carboxylic acid derivatives in the rat aortic ring model cause NO-dependent releasing properties through a mechanism involving the NO signaling pathway, as supported by the inhibitory effects of the guanylate cyclase inhibitor methylene blue. The former exhibited enhanced NO-dependent releasing properties relative to the latter. It should be stressed that only hydroxamic acid derivatives, *via* the hydroxamic acid functional group, have the potential to

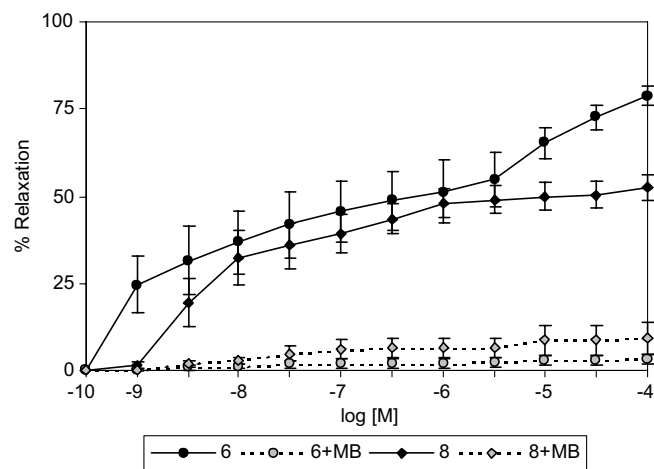


Fig. 9. Effects of *cis*-[Pt^{II}Cl₂(3-pycaH)₂] (**6**) and *cis*-[Pt^{II}Cl₂(3-pycaH)₂] (**8**) in the presence or absence of methylene blue (MB).

release NO. It may therefore be hypothesised that the mechanism of vasorelaxation of aortic rings is probably due to stimulation of NOS activity of the aorta endothelial cells, to which NO-release from compounds **6** and **7** might also contribute, at least at concentrations higher than 3×10^{-5} M.

4. Conclusions

A series of novel Pt^{II} and Pt^{IV} pyridinehydroxamic acid complexes were synthesised with a view to advancing a new class of metallodrug with dual DNA-binding and NO-releasing properties. We can conclude from our investigation that the Pt^{II} pyridinehydroxamic acid derivatives induce potent *in vitro* effects attributable to either NO-release from the hydroxamic acid moiety and/or stimulation of iNOS of the endothelial cells. Considering the role of NO and iNOS activation in the process of proliferation and metastases, the data of the present work suggest further *in vitro* and *in vivo* testing of these compounds on cell proliferation and solid metastasising tumours, respectively. The complexes herein described are not however sufficiently soluble for a full biological investigation. We are currently in the process of developing analogues with superior aqueous solubility.

Acknowledgements

The authors thank Enterprise Ireland under its Basic Research Grant Programme and International Collaboration Scheme, EU COST D20, EU COST D39 and the Programme for Research in Third Level Institutions (PRTL), administered by the HEA for funding. MADE project at Callerio Foundation is also acknowledged for support. We thank Dr. Dilip Rai (School of Chemistry and Chemical Biology, Science Education and Research Centre, UCD, Belfield, Dublin 4, Ireland) for MS analysis. C.J.M. gratefully acknowledges Johnson Matthey for the generous loan of K₂[Pt^{II}Cl₄] and K₂[Pt^{IV}Cl₆].

Appendix A. Supplementary material

CCDC 251892 contains the supplementary spectroscopic data for **1–4** and **6–14** and the crystallographic data for **12**. These data can be obtained free of charge via <http://www.ccdc.cam.ac.uk/conts/retrieving.html>, or from the Cambridge Crystallographic Data Centre, 12 Union Road, Cambridge CB2 1EZ, UK; fax: (+44) 1223-336-033; or e-mail: deposit@ccdc.cam.ac.uk. Supplementary data associated with this article can be found, in the online version, at [doi:10.1016/j.poly.2007.03.011](https://doi.org/10.1016/j.poly.2007.03.011).

References

- [1] M. Galanski, M.A. Jakupc, B.K. Keppler, *Curr. Med. Chem.* 12 (2005) 2075, and references therein.
- [2] A.S. Abu-Surrah, M. Kettunen, *Curr. Med. Chem.* 13 (2006) 1337, and references therein.
- [3] S. van Zutphen, J. Reedijk, *Coord. Chem. Rev.* 249 (2005) 2845.
- [4] G. Natile, M. Coluccia, *Met. Ions Biol. Syst.* 42 (2004) 209.
- [5] N. Farrell, *Met. Ions Biol. Syst.* 42 (2004) 251.
- [6] B.A. Jansen, P. Wielaard, G.V. Kalayda, M. Ferrari, C. Molenaar, H.J. Tanke, J. Brouwer, J. Reedijk, *J. Biol. Inorg. Chem.* 9 (2004) 403.
- [7] M.D. Hall, R.C. Dolman, T.W. Hambley, *Met. Ions Biol. Syst.* 42 (2004) 297.
- [8] C. Napoli, L.J. Ignarro, *Annu. Rev. Pharmacol. Toxicol.* 43 (2003) 97.
- [9] C.J. Marmion, B. Cameron, C. Mulcahy, S.P. Fricker, *Curr. Top. Med. Chem.* 4 (2004) 1585, and references therein.
- [10] B. Bonavida, S. Khineche, S. Huerta-Yepez, H. Garban, *Drug Resist. Update* 9 (2006) 157.
- [11] L. Morbidelli, S. Donnini, M. Ziche, *Curr. Pharm. Des.* 9 (2003) 521.
- [12] C. Bogdan, *Nat. Immunol.* 2 (2001) 907.
- [13] S.P. Fricker, *Platinum Met. Rev.* 39 (1995) 150.
- [14] C. Szabo, H. Ohshima, *Nitric Oxide* 1 (1997) 373.
- [15] W. Xu, L.Z. Liu, M. Loizidou, M. Ahmed, I.G. Charles, *Cell Res.* 12 (2002) 311.
- [16] G.R. Thatcher, *Curr. Top. Med. Chem.* 5 (2005) 597.
- [17] R. Scatena, P. Bottoni, G.E. Martorana, B. Giardina, *Expert Opin. Invest. Drugs* 14 (2005) 835.
- [18] C.J. Marmion, T. Murphy, J.R. Docherty, K.B. Nolan, *Chem. Commun.* (2000) 1153.
- [19] C.J. Marmion, D. Griffith, K.B. Nolan, *Eur. J. Inorg. Chem.* 15 (2004) 3003, and references therein.
- [20] E. Alessio, G. Mestroni, A. Bergamo, G. Sava, *Curr. Top. Med. Chem.* 4 (2004) 1525.
- [21] M.J. Clarke, *Coord. Chem. Rev.* 236 (2003) 209.
- [22] D. Griffith, E. Zangrando, E. Alessio, C.J. Marmion, *Inorg. Chim. Acta* 357 (2004) 3770.
- [23] K. Karidi, A. Garoufis, A. Tsipis, N. Hadjiliadis, H. den Dulk, J. Reedijk, *Dalton Trans.* 7 (2005) 1176.
- [24] N.P. Konovalova, S.A. Goncharova, L.M. Volkova, T.A. Rajewskaya, L.T. Eremenko, A.M. Korolev, *Nitric Oxide* 8 (2003) 59.
- [25] J. Comiskey, E. Farkas, K.A. Krot-Lacina, R.G. Pritchard, C.A. McAuliffe (the late), K.B. Nolan, *Dalton Trans.* (2003) 4243.
- [26] G.M. Sheldrick, University of Göttingen, 1997.
- [27] C.M. Hu, J.J. Kang, C.C. Lee, C.H. Li, J.W. Liao, Y.W. Cheng, *Eur. J. Pharmacol.* 468 (2003) 37.
- [28] B. van't Riet, G.L. Wampler, H.L. Elford, *J. Med. Chem.* 22 (1979) 589.
- [29] D.A. Brown, R.A. Coogan, N.J. Fitzpatrick, W.K. Glass, D.E. Abukshima, L. Shiels, M. Ahlgren, K. Smolander, T.T. Pakkanen, T.A. Pakkanen, M. Perakyla, *J. Chem. Soc., Perkin Trans. 2* (1996) 2673.
- [30] C. Mulcahy, F.M. Dolgushin, K.A. Krot, D. Griffith, C.J. Marmion, *Dalton Trans.* (2005) 1993.
- [31] N. Farrell, L.R. Kelland, J.D. Roberts, M. Van Beusichem, *Cancer Res.* 52 (1992) 5065.
- [32] J. Arpalahiti, B. Lippert, *Inorg. Chim. Acta* 138 (1987) 171.
- [33] K. Nakamoto, *Infrared and Raman Spectra of Inorganic and Coordination Compounds*, 4th ed., Wiley, New York, 1986.
- [34] A.A. Diamantis, J.V. Dubrawski, *Inorg. Chem.* 20 (1981) 1142.